

Supplementary Materials for
NRF2 controls iron homeostasis and ferroptosis through HERC2 and VAMP8

Annadurai Anandhan *et al.*

Corresponding author: Email: zhangd@arizona.edu

Sci. Adv. 9, eade9585 (2023)
DOI: 10.1126/sciadv.ade9585

This PDF file includes:

Figs. S1 to S6

SUPPLEMENTAL FIGURES:

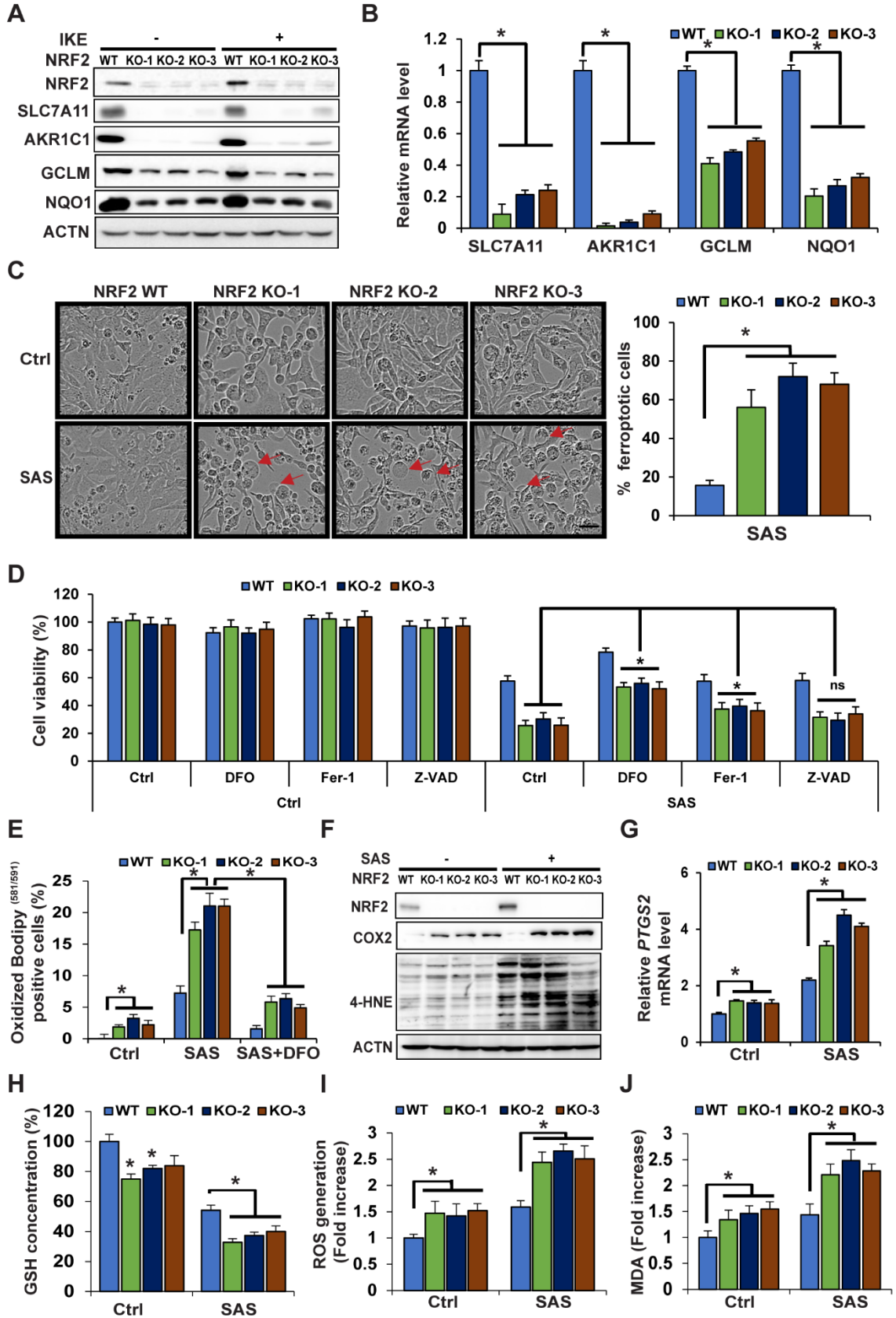


Figure S1. *NFE2L2/NRF2* deletion sensitizes ovarian cancer cells to ferroptosis, related to Figure 1. (A-B) Three out of >10 individual *NFE2L2/NRF2* knockout (KO) SKOV-3 ovarian cancer cell lines established using CRISPR-Cas9 gene editing were chosen for further study. Cells were left untreated or treated with IKE (10 μ M) for 12 h. (A) Cell lysates were collected for immunoblot analysis of NRF2 and its target genes, or (B) for qRT-PCR analysis of the mRNA levels of the indicated NRF2 target genes. (C) Ferroptotic cell morphology (ballooning) following sulfasalazine (SAS) treatment (2.5 mM, 24 h) was visualized using the Incucyte imaging system (left panel). Over 1000 cells were counted and the percentage of ferroptotic cells was plotted (right panel). Scale bar = 50 μ m. (D) *NFE2L2/NRF2* WT and KO cell lines were treated with DFO (100 μ M), Fer-1 (10 μ M), or Z-VAD-fmk (20 μ M); alone with DMSO or SAS (2.5 mM) for 24 h. Cell viability was measured by MTT assay. (E-J) These four cell lines were treated with 2.5 mM SAS for 12 h before the following endpoints were measured: (E) lipid peroxide production was assessed by flow cytometry using C11-BODIPY^{581/591}. DFO co-treatment: 100 μ M, 12 h. (F) 4-hydroxynonenal (4-HNE)-protein adducts and COX2 protein levels were measured by immunoblot analysis. (G) mRNA levels of *PTGS2* were measured by qRT-PCR. (H) Total intracellular glutathione (GSH) levels were measured by the QuantiChrom glutathione assay. (I) ROS were measured by electron paramagnetic resonance (EPR) spectroscopy. (J) Malondialdehyde (MDA) formation was detected colorimetrically using the thiobarbituric acid reactive substances (TBARS) assay. Data are represented as mean \pm SEM of three biological replicates. (n=3), *p<0.05.

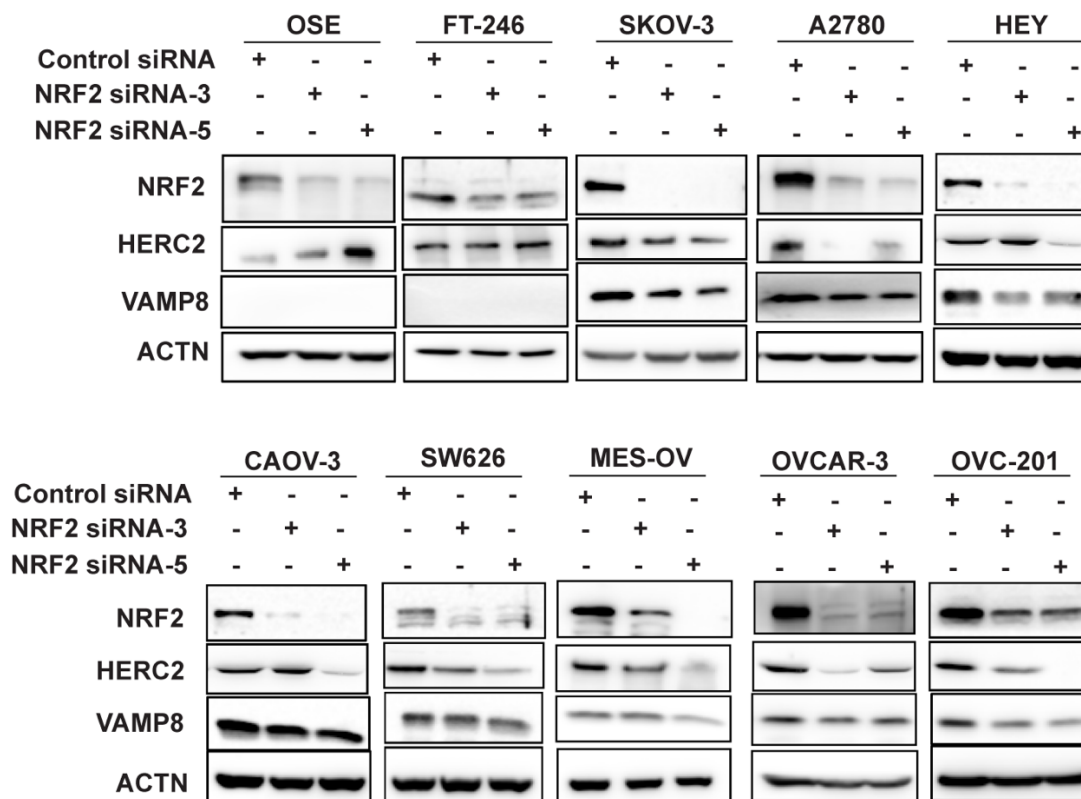


Figure S2. *HERC2*, an E3 ubiquitin ligase for *FBXL5* and *NCOA4*, is an *NRF2* target gene, related to Figure 3. Immortalized normal ovarian surface epithelial (OSE)¹ and fallopian tube (FT-246)² cell lines, as well as several ovarian cancer cell lines (SKOV-3, A2780, HEY, CAOV-3, SW626, MES-OV, OVCAR-3, and OVC-201) were transfected for 72 h with two different *NRF2*-siRNAs, or a control siRNA (10 nM). Cell lysates were used for immunoblot analysis of *NRF2*, *HERC2*, *VAMP8* and β -actin.

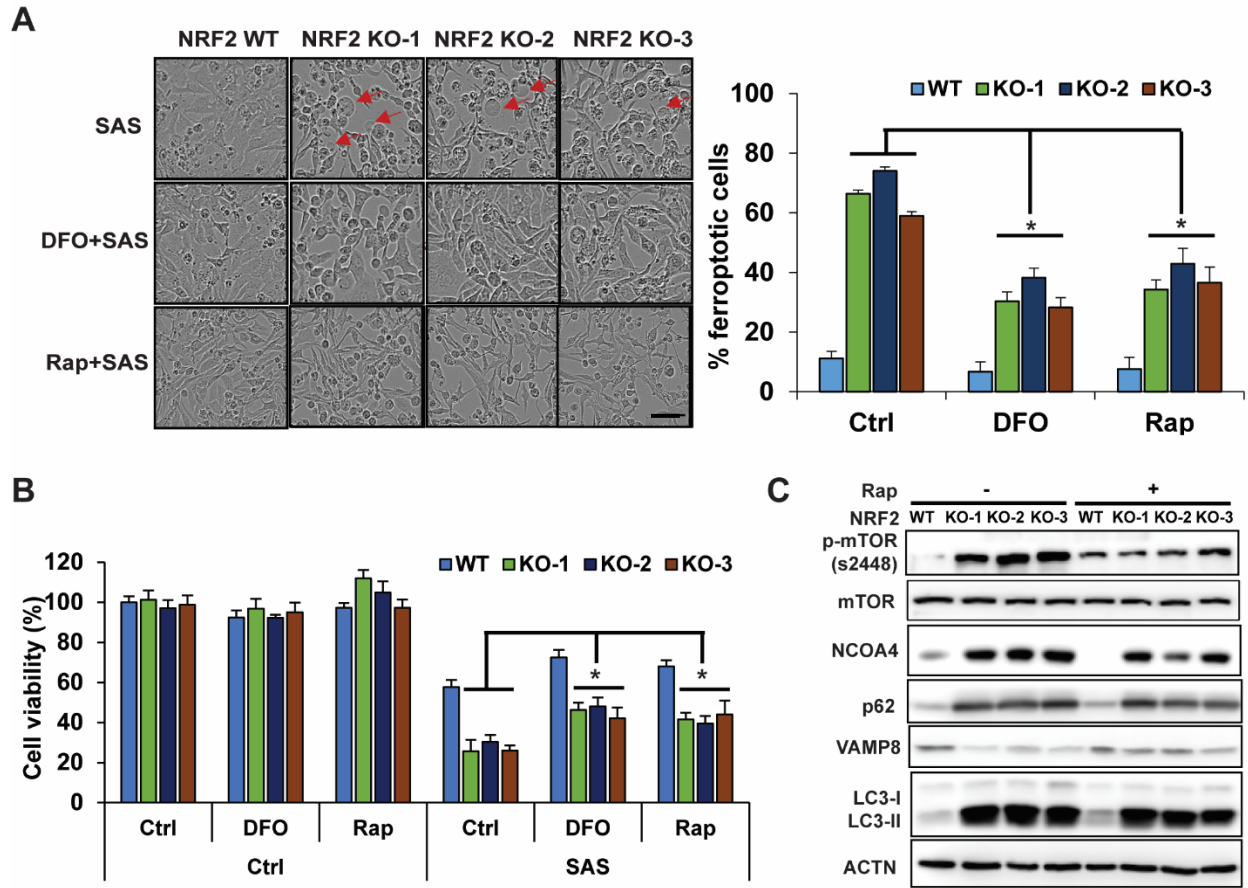


Figure S3: DFO and rapamycin treatment partially prevent sulfasalazine-induced ferroptosis in NRF2 KO ovarian cancer cells, related to Figure 3. SKOV3 *NFE2L2*/WT and KO cells were pre-treated with deferoxamine (100 μ M), or rapamycin (1 μ M) for 1h before the cells were treated with 2.5 mM sulfasalazine (SAS) for an additional 24h. (A) Cell images were captured using the IncuCyte system (left panel). Ferroptotic cells were identified based on ferroptotic cell morphology (ballooning). Over 1000 cells were counted and the percentage of ferroptotic cells was plotted (right panel). Scale bar = 50 μ m. (B) Cell viability was measured by MTT assay. (C) The indicated proteins were detected by immunoblot analysis.

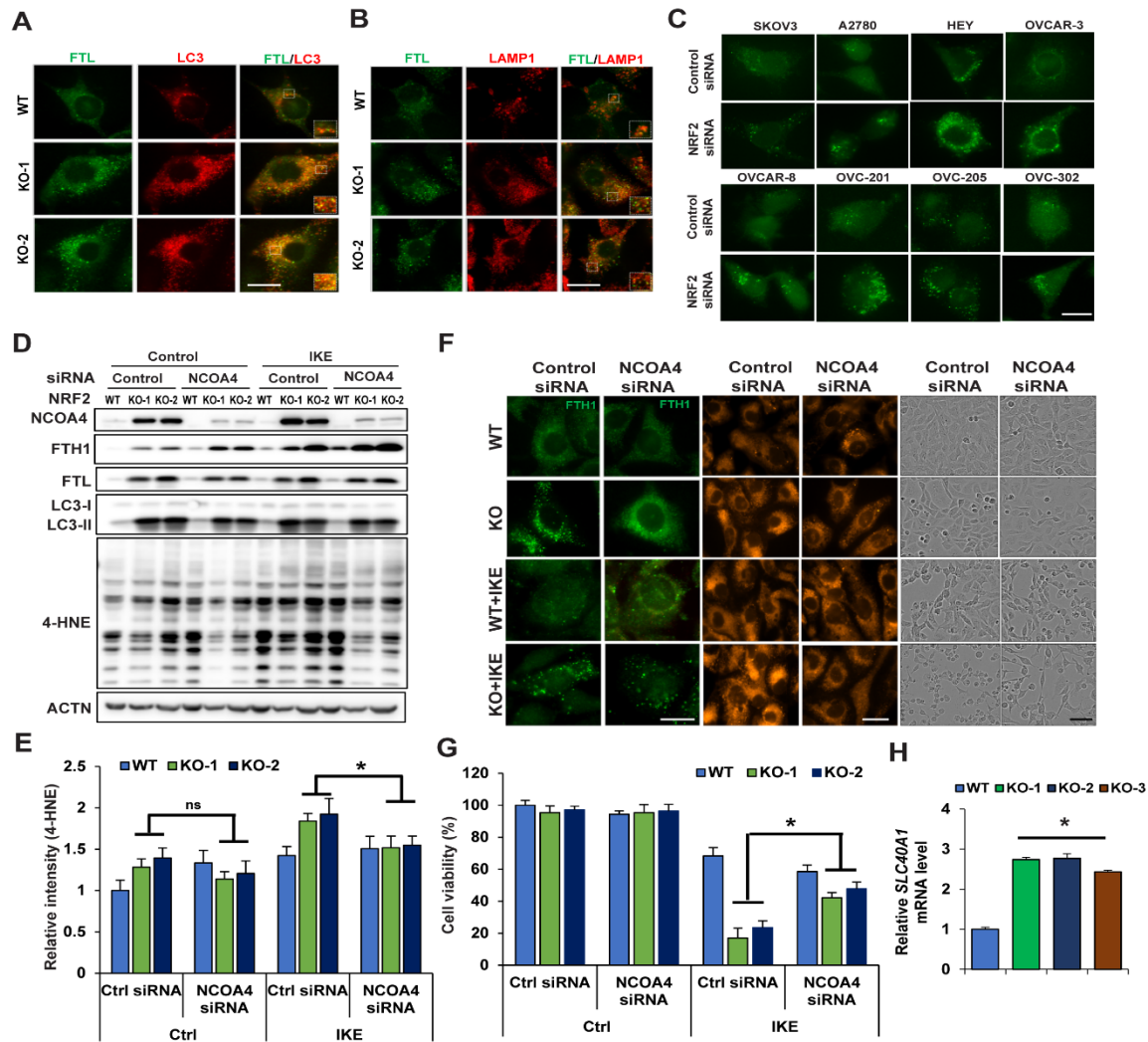


Figure S4. Inhibition of ferritinophagy in *NFE2L2/NRF2* KO cells leads to autophagosomal accumulation of apoferritin/NCOA4, increased LIP, and enhanced sensitivity to ferroptotic cell death, related to Figure 5. (A-B) Indirect immunofluorescence analysis of (A) FTL and LC3, and (B) FTL and LAMP1 in *NFE2L2/NRF2* WT or *NFE2L2/NRF2* KO SKOV-3 cell lines. Inset shows magnified puncta. (C) Several established ovarian cancer cell lines (SKOV-3, A2780, HEY, OVCAR-3, OVCAR-8, OVC-201, OVC-205, and OVC-302.) were transfected for 72 h with an *NFE2L2/NRF2*-siRNA or control-siRNA (10 nM), followed by indirect immunofluorescence analysis of FTH1 puncta. Scale bar = 10 μ m. (D) Protein levels of FTH1, FTL, LC3 I/II, and 4-HNE adducts in *NFE2L2/NRF2* WT and KO cells transfected with control siRNA or *NCOA4* siRNA for 72 h, IKE (10 μ M) was added 12 h before harvest. (E) Quantification of 4-HNE adduct levels of the immunoblot in D. (F) (Left panels) FTH1 indirect immunofluorescence (Scale bar = 10 μ m.); (Middle panels) LIP (Fe^{2+}) as measured by FerroOrange immunofluorescence (Scale bar = 25 μ m.); and (Right panels) Ferroptotic cell morphology following *NCOA4* knockdown for 72 h and IKE treatment (10 μ M, 24 h; Scale bar = 50 μ m). (G) Cell viability following *NCOA4* knockdown for 72 h and IKE treatment (10 μ M, 24 h), as measured by MTT assay. (H) Relative mRNA levels of *SLC40A1* in *NFE2L2/NRF2* WT versus KO cells.

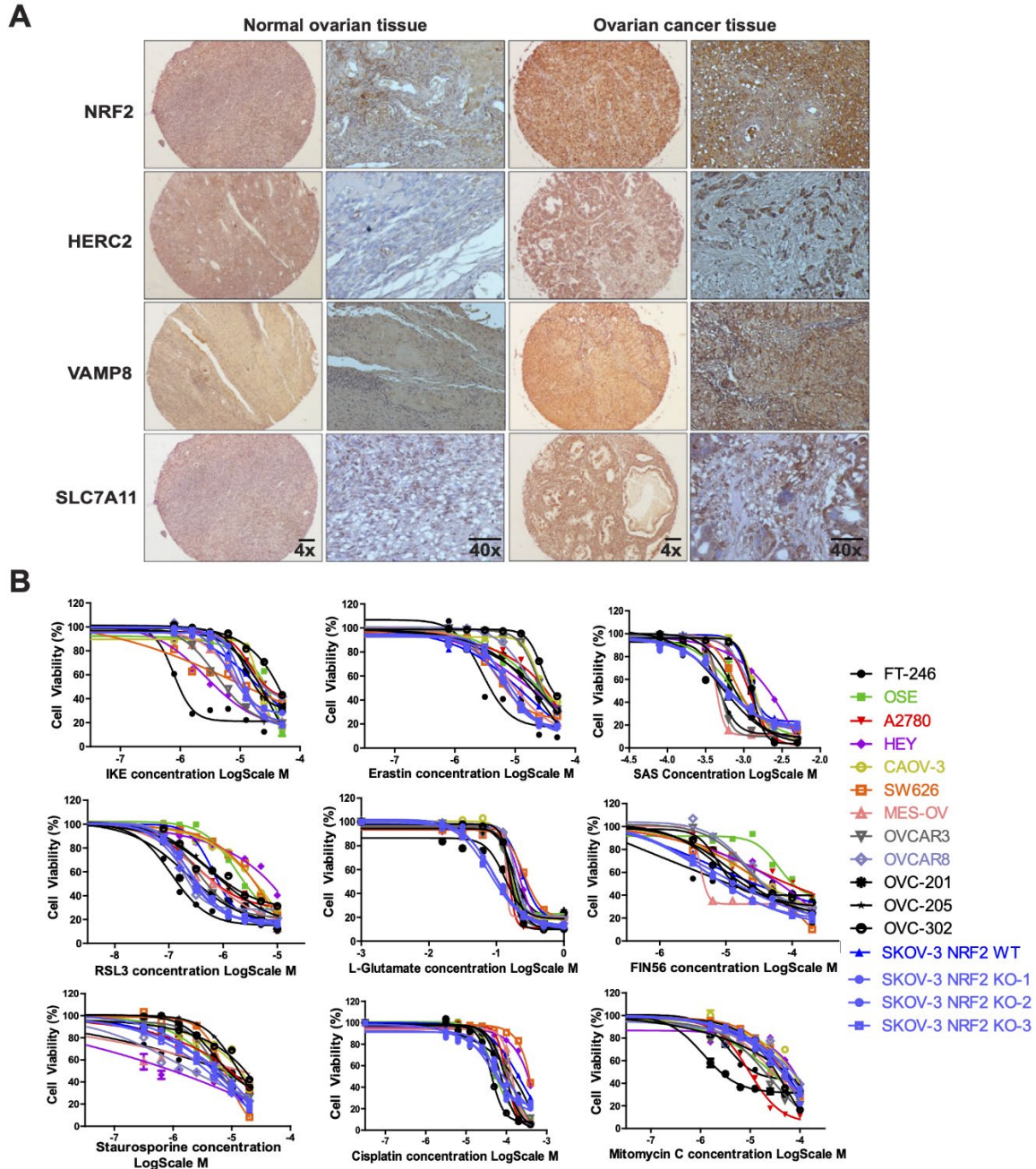


Figure S5. NRF2 expression correlates with HERC2 and VAMP8 levels in human cancer tissues, as well as ferroptosis resistance, related to Figure 6 . (A) Correlation between NRF2 expression and HERC2 or VAMP8 levels in human ovarian tissues was determined by immunohistochemistry analysis. HERC2, VAMP8, and SLC7A11 expression were imaged, and average intensity was measured and plotted against NRF2 (images in Figure S4A, protein expression correlation dots of individual patients in Figure 6A). Normal tissue (n=10); cancer tissue (n=40). 4X scale bar = 100 μ m; 40X scale bar = 20 μ m. (B) Each of the indicated ovarian cell lines was treated with eight doses of the indicated compound for 24 h, and cell viability was measured by MTT assay and plotted to obtain a CC₅₀ value (Also see Table S3).

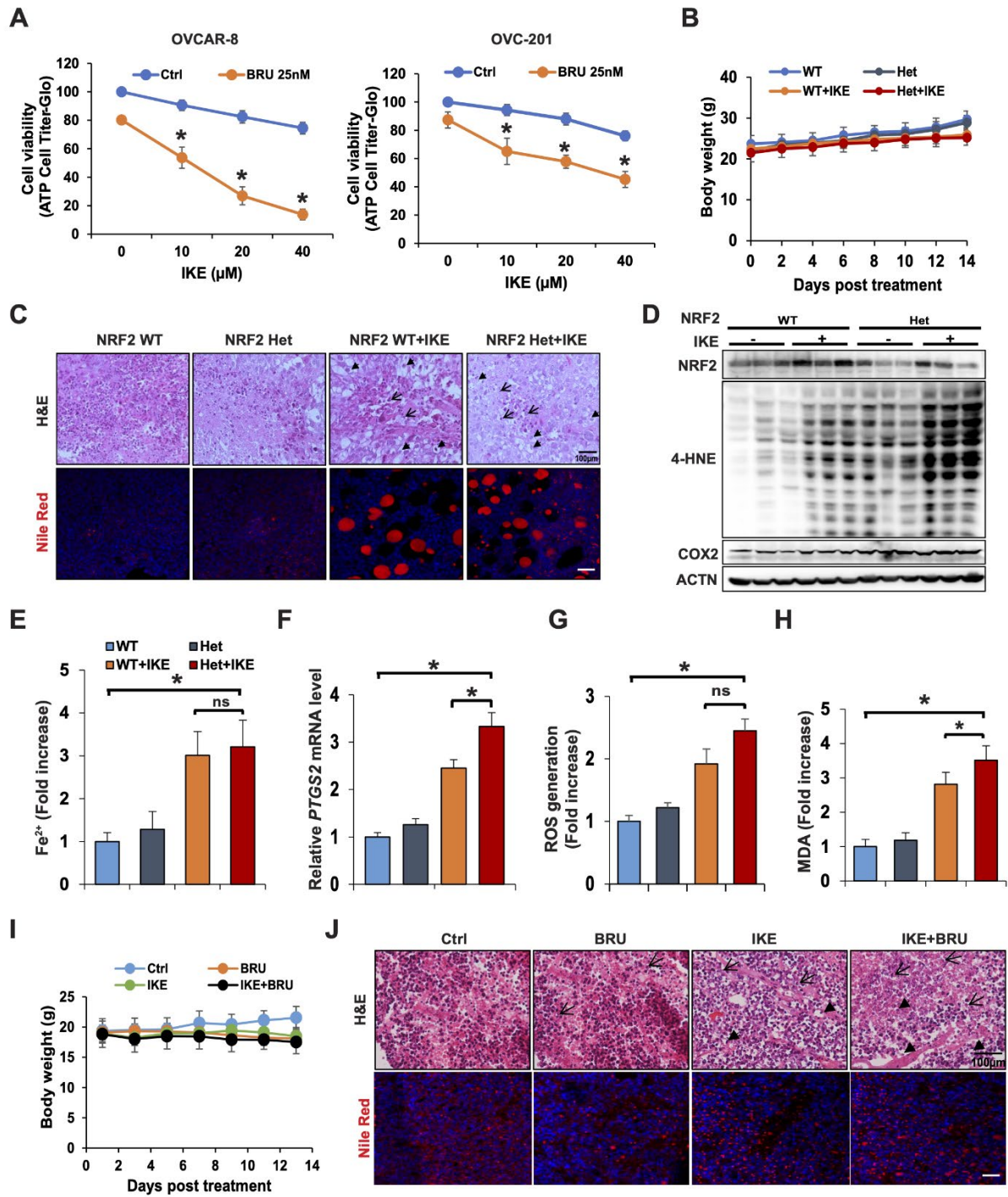


Figure S6. Genetic ablation or pharmacological inhibition of NRF2 enhanced sensitivity to ferroptotic cell death in four preclinical models, related to Figure 7

(A) OVCAR-8 and OVC-201 cells were seeded into each well of a hanging drop array plate and grown until 3D spheroids were formed. Cell viability of these cell lines treated with several dose of IKE in the absence or presence of brusatol (20 nM) at 24 h time point was assessed by Cell Titer-Glo assay. * $p < 0.05$, $n = 8$. (B) Bodyweight of NSG mice bearing *NFE2L2/NRF2* WT or Het xenograft tumors IP injected with vehicle control or 40 mg/kg IKE daily for 14 days, as described in Figure 7C. * $p < 0.05$, $n = 15$ /group. (C) H&E and Nile

Red staining of *NFE2L2/NRF2* WT and Het xenograft tumor tissues. Scale bar = 100 μm . (D) 4-hydroxynonenal (4-HNE)-protein adducts and COX2 protein levels in the tumor tissues were measured by immunoblot analysis. (E) LIP (Fe^{2+}) in these tumor tissues was measured by colorimetric assay using Ferene-S. * $p < 0.05$, $n = 6$. (F) mRNA levels of *PTGS2* in the tumor tissues were measured by qRT-PCR. * $p < 0.05$, $n = 6$. (G) ROS in tumor tissues were measured by electron paramagnetic resonance (EPR) spectroscopy. * $p < 0.05$, $n = 6$. (H) Malondialdehyde (MDA) formation in tumor tissues was detected colorimetrically using the TBARS assay. * $p < 0.05$, $n = 8$. Data are represented as mean \pm SEM of tumor tissues ($n = 6$) from six individual mice. (I) Body weight of NSG mice implanted with PDX tumor tissues and treated with vehicle control, Bru (0.25 mg/kg), IKE (20 mg/kg), or IKE + Bru daily for 14 days, related to Figure 7F. * $p < 0.05$, $n = 10/\text{group}$. (J) H&E and Nile Red staining of PDX tumor tissues, related to Figure 7F. Scale bar = 100 μm .